

Reply to Reviewer Comments

General comments

In this brief communication the authors present the results of a Sentinel-1-based automated near-real time flood mapping approach applied for detecting inundations caused in the frame of Hurricane Dorian on the Bahamas. Even if the inundations on the Bahamas were huge and very impressive the most important limitations of the work are in my view 1) the sole application of an already reported approach to a small subset of existing data sets which had been acquired over the Bahamas during this event, 2) the missing validation of the flood mapping results and 3) the lack of consideration of the work of other authors which achieved significant progress in SAR-based flood mapping within the last years.

We would like to thank the reviewer for his/her constructive comments. We have revised the paper according to all the reviewer's comments, and we are detailing our response (in green) in this document.

- 1) The reviewer is correct in stating that this paper discusses about a sole application of an already reported approach. However, this is the first times that this algorithm has been used in near-real time during an event, being now fully-automated. For these reasons, we chose the "Brief Communication" format to timely "disseminate information and data on topical events of significant scientific and/or social interest within the scope of the journal". In order to publish timely results, we did not test the case using all existing methods and we will argue in a following response that it is unnecessary to do so.
- 2) The RAPID system has been quantitatively validated using different methods by (Shen et al. 2019a) and (Yang et al. 2019) in different events and locations against different reference datasets. In the revised version of the manuscript we are reporting the accuracy values from the validation performed in those studies. Since RAPID has been thoroughly validated by other studies, this paper is a brief communication about the Bahamas inundation instead of the system development. Furthermore, we cannot find an independent third-party reference flood map extend to validate the estimates from the RAPID system. There are flood maps for September 2 and September 4, 2019 derived by ESA/EMS, but those are based on the same SAR observations. We included, in the new version of our manuscript, a comparison with these EMS maps.
- 3) Thank you for raising this point. The work of other authors had been extensively discussed in (Shen et al., 2019a) and (Shen et al., 2019b). Unfortunately, due to the nature of this paper, it cannot contain an extensive literature review. In the previous version of this manuscript we chose to cite only all the data sources used, and the work at the basis of this manuscript. In the revised version we also include some of the most important papers written by other authors: "*Only a few SAR-based flood delineation methods (e.g. Horritt et al. 2003, Martinis et al. 2009, Matgen et al., 2011, Giustarini et al. 2012, Lu et al. 2014, Chini et al. 2017, Cian et al. 2018) have the potential to be fully automated (Shen et al. 2019b).*" However, we would like to point out that although many algorithms claim a certain level of automation, they are limited in applications. For example, some method require bimodal histogram, while other are based on simple threshold-based methods suffering by over-detection of artificial surfaces. Most methods cannot directly be applied without human interference. The RAPID system overcomes all these issues and is the only system that requires no human interference from the identification of potential flooded areas to the final generation of flood maps from SAR. We retrospectively outputted all Sentinel-1 captured flood events in the CONUS area from 2016 to 2019, which is the main contribution of (Yang et al. 2019). Since the RAPID system, being fully automated, is more automated than other existing system, we 1) were the first to release the Bahamas flood maps to the public (half day

earlier than Copernicus/EMS), and 2) did not only map selected events of high impact or the peak of the selected event, but also reported every captured event in the CONUS area and every captured day in an event.

Specific comments

1. Abstract: In my view the focus of this contribution is not clear. The method for detecting flooding based on SAR data is already published by the authors and, as this is a brief communication, there is of course only shortly reported on the details of the methodology. Therefore, the focus of this publication should be on the huge flood event on the Bahamas. However, only Sentinel-1 data on two dates in early September has been analysed. By integrating other Earth Observation data sets acquired during this event (e.g. in the frame of the International Charter Space and Major Disasters) and also additional Sentinel-1 data acquired in September 2019 (e.g. on September 14) the evolution of this flood event could be better described (the RAPID approach could be of course a component to complete the description of this event).

Thank you for this comment. We agree with the reviewer about the clarity of the focus of our paper. In particular, we are not presenting the methodology for an automated system, but we are presenting the application of that system. For this reason we modified the following sentence of the abstract by adding the words “an application of”:

“we present an application of the automated near-real-time (NRT) system called RADar-Produced Inundation Diary (RAPID) to European Space Agency Sentinel-1 SAR images to produce flooding maps for Hurricane Dorian in the northern Bahamas.”

The reviewer’s question related to other Earth Observation data may arise by our lack of specificity on the resolution. In the previous version of the manuscript we generically wrote about “high-resolution”. However, the resolution of this product is much higher than other high-resolution products: it is 10 meters (we included this information in the current version). Most of the other products are either at a lower resolution, or optical. Optical sensors do not work in adverse weather conditions and are not reliable for an immediate response to hurricanes. To make this difference clear, we added the following sentence in the paper:

“Differently than optical sensors, SAR images are not influenced by adverse weather conditions.”

Moreover, in the revised version we now include a comparison with the EMS product (which is based on the same SAR observation) in Figure 2, in the new Table 1, and in text:

“The agreement (overall, user, producer) scores between RAPID and EMS flooding maps for the Abaco Islands on September 2 and September 4, derived from the confusion matrix shown in Table 1, were (77%, 90%, 41%) and (89%, 61%, 86%), respectively. The high overall and user agreement scores for the September 2 flooding are also depicted in the flood maps of Figure 2 indicating a very good overlap of the two products over the coast of Great Abaco, while the relatively low producer agreement comes from the lack of flood detection by the EMS algorithm over the multiple near-sea-surface-elevation islands, located in the front of the western coast of Great Abaco. The relatively low user agreement score between the two products on September 4 is due to the fact that RAPID classifies some non-flooded areas within the EMS flooded boundary, which are expected to occur as a consequence of the flood recession.”

Flooding retreat and comparison between RAPID and EMS

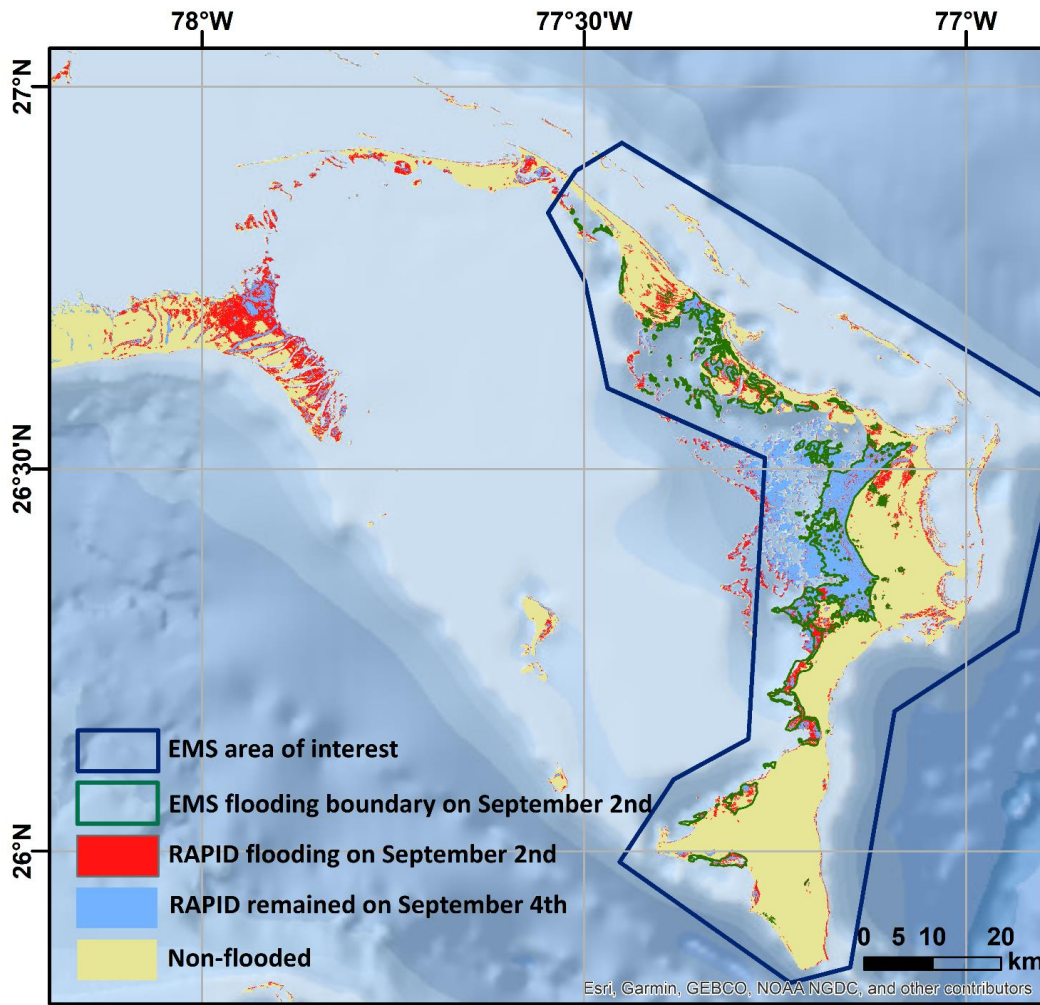


Figure 2: Ocean background from World Ocean Base map (ESRI et al. 2014; list of contributors available at: http://downloads.esri.com/esri_content_doc/da/WorldOcean_ContributorsDA64.pdf). Flooded and non-flooded areas on September 2 and September 4, 2019 derived from the RAPID algorithm that processed SAR data from the Sentinel-1 overpasses, and flooded boundary from EMS.

Confusion Matrix		September 2 – Great Abaco		September 4 – Grand Bahama	
		Flooded	Non-flooded	Flooded	Non-flooded
RAPID	Flooded	2,274,927 (14.5%)	3,318,143 (21.1%)	1,880,609 (13.2%)	32,989 (2.3%)
	Non-flooded	260,335 (1.7%)	9,847,017 (62.7%)	1,219,786 (8.6%)	10,710,519 (75.9%)

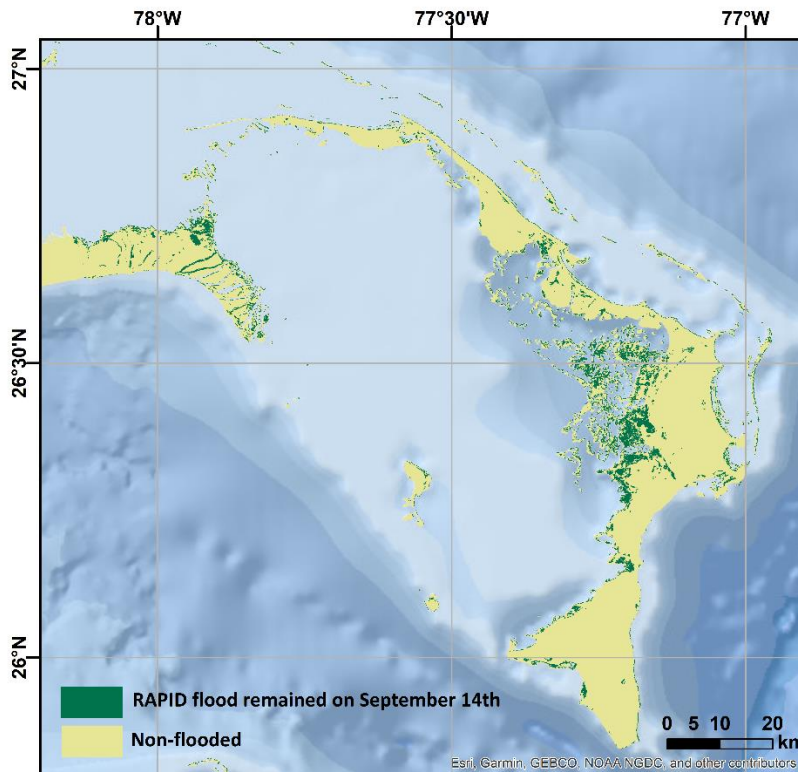
Table 1: Confusion matrix between RAPID and EMS flooding products for September 2, 2019 overpass over Great Abaco (left) and for September 4, 2019 overpass over Grand Bahama (right). For each matrix, number and percentage of pixels is reported.

We also mentioned visible products available on the International Charter Space and Major Disasters website, which confirm the results we found for Andros Island:

“RAPID flooding estimates of area and inland extent on the Andros Island are in agreement with the coarser resolution product composited from VIIRS (375m) and ABI (1km) passive radiometers, displayed on the International Charter “Space and Major Disasters” website at https://disasterscharter.org/image/journal/article.jpg?img_id=3519568&t=1568272371731.”

Finally, we would like to mention that the September 14 image, being acquired more than 10 days after the passage of the hurricane, shows just a very limited amount of flooded area. We believe it is not necessary to include this image in the brief communication.

Flooding remained on Sep.14th, Bahamas



2. Line 38: Please replace Alos-2 by ALOS-2/PALSAR-2

Thank you for this comment. We replaced Alos-2 with ALOS-2/PALSAR-2 in the revised manuscript.

3. Line 43: There exist several automatic approaches/complete processing chains for detecting flood extent from different kind of radar satellite data (e.g. from TerraSAR-X, Sentinel-1, CosmoSkyMed). Multiple references have been published related to this topic within the last years by different organisations. Some of these references should be cited in this publication.

The combined methods that can provide a complete processing for detecting flood extent from different kind of radar satellite data have been discussed in “Inundation Extent Mapping by Synthetic Aperture Radar: A Review” by Shen et al., 2019, which reads as follows:

“Martinis et al. (2009) applied SBA –split-based approach- (Bovolo and Bruzzone 2007) to determine the global threshold for binary (water and non-water) classification. In SBA, a SAR image is first divided into splits (sub-tiles) to determine their individual thresholds using the Kittler and Illingworth (KI) method (Kittler and Illingworth 1986), global minimum, and quality index. Then, only qualified splits showing sufficient water and non-water pixels are selected to get the global threshold. The OO segmentation algorithm (implemented in e-cognition software) is used to segment the image into continuous and non-overlapping object patches at different scales. Then the global threshold is applied to each object. Eventually, topography is used as an option to fine-tune the results.

SBA is employed to deal with the heterogeneity of SAR backscattering from the same object in time and space. The intention of applying the OO segmentation algorithm is to reduce false alarms and speckle noise. OO was, however, originally designed for high-resolution optical sensors, which have no consideration of noise like speckle and water-like areas. The fine-tuning procedure can only deal with floodplain extended from identified water bodies, leaving inundated areas isolated from known water sources. To avoid the drawback of fixing tile size to SAR images of different places and resolution (Bovolo and Bruzzone 2007; Martinis et al. 2015; Martinis et al. 2009), Chini et al. (2017) propose the hierarchical SBA (HSBA) method with variable tile size, and they post-processed the binary water mask derived by HSBA using RGA and CD, similar to Giustarini et al. (2013); Matgen et al. (2011).

The ACM, also known as the snake algorithm (Horritt 1999), was, to the authors’ knowledge, the first image segmentation algorithm designed for SAR data. It allows a certain amount of backscattering heterogeneity, while no smoothing across segment boundaries occurs. A smooth contour is favored by the inclusion of curvature and tension constraint. The algorithm spawns smaller snakes to represent multiple connected regions. The snake starts as a narrow strip moving along the course of a river channel, ensuring it contains only flooded pixels. Overall, it can deal with low signal to noise ratio.

Horritt et al. (2003) used ACM to map waterlines under vegetation. They started from known pure ocean pixels to map the active contour of open water and then to map the second active contour, which was the waterline beneath vegetation. Two radar signatures—the enhanced backscattering at C-band and the HH-VV phase difference at L-band—forced the ACM. Unlike the OO method, which aggregates objects from the bottom (pixel level) to the top, the segmentation in ACM requires seeding pixels, whose detection is difficult in an automated approach. In addition, similar to RGA, ACM cannot detect inundated areas isolated from a known water body.”

In our manuscript, we modified the first sentence in the Methodology section for including the above and additional references:

“Only a few SAR-based flood delineation methods (e.g. Horritt et al. 2003, Martinis et al. 2009, Matgen et al., 2011, Giustarini et al. 2013, Lu et al. 2014, Chini et al. 2017, Cian et al. 2018) have the potential to be fully automated (Shen et al. 2019b).”

However, we would like to mention that, to the authors’ knowledge, Sentinel-1 is the only open data that is frequently available globally. In our paper we are only comparing Sentinel-1 based flood mapping results since satellites mentioned by the reviewer are not accessible by everyone including the authors.

4. Line 54: It would be better to cite directly the references related to automated flood delineation and not to refer only to previous work of the authors (Shen et al. 2019b)

Thank you for this comment. We are now citing directly the references related to automated flood delineation:

“Only a few SAR-based flood delineation methods (e.g. Horritt et al. 2003, Martinis et al. 2009, Matgen et al., 2011, Giustarini et al. 2013, Lu et al. 2014, Chini et al. 2017, Cian et al. 2018) have the potential to be fully automated (Shen et al. 2019b).”

Also in this case, for a detailed literature review, we are still referring to Shen et al. 2019b, which reads as follows:

“Toward automation, Matgen et al. (2011) developed the M2a algorithm to determine the threshold that makes the non-water pixels (below the threshold) best fit a gamma distribution—a theoretical distribution of any given class in a SAR image. They then extended flooded areas using RGA from detected water pixels using a larger threshold—99 percentile of the “water” backscatter gamma distribution—arguing that flood maps resulting from region growing should include all “open water” pixels connected to the seeds. Then they applied a change detection technique to backscattering to reduce over-detection within the identified water bodies caused by water-like surfaces, as well as to remove permanent water pixels.

Based on the same concept, Giustarini et al. (2013) developed an iterative approach to calibrate the segmentation threshold, distribution parameter, and region growing threshold (M2b). They applied the same segmentation threshold to the dry reference SAR image to obtain the permanent water area. They claimed, however, that if the intensity distribution of the SAR image were not bimodal, the automated threshold determination might not work.

Lu et al. (2014) used a changed detection approach, first to detect a core flood area that contained a more plausible but incomplete collection of flood pixels, and then to derive the statistical curve of the water class to segment water pixels. The major advantage of this approach is that a bimodal distribution is not compulsory. In practice, a non-bimodal distribution often occurs. The change detection threshold might be difficult to determine and globalize.

Assuming even prior probability of flooded and non-flooded conditions, Giustarini et al. (2016) computed probabilistic flood maps that characterize the uncertainty of flood delineation. The probability reported in this study, however, related to the uncertainty neither in extent nor in time. Rather, it was the uncertainty of a SAR image classification based on backscattering.

Taking advantage of big earth observation (EO) data, the two most recent studies—Cian et al. (2018) and Shen et al. (2019)—implemented full automation of inundation retrieval. With the CD principle underpinning both methods, they employed multiple dry references instead of one supported by operational satellite SAR data for multiple years.

Cian et al. (2018) developed two CD-based flood indices, the Normalized Difference Flood Index (NDFI) and the Normalized Difference Vegetated Flood Index (NDVFI), assuming a number of revisits for each pixel in dry conditions was available.”

5. Line 65: It should be at least mentioned which Sentinel-1 data type (GRD or SLC) and polarization is used for extracting the flooding

Thank you. The Sentinel- data type is GRD and RAPID uses both channels in the dual polarization modes but could also work if occasionally single polarization or fully polarization data were provided. We added this information in the revised version:

“the RAPID core algorithm (Shen et al. 2019a) handles both polarizations of SAR images in GRD mode through four steps”.

6. Result section: It would be important to perform an accuracy assessment of the flood masks

As responded in our item 2 to the general comments, for Bahamas, it is difficult to find another fully independent reference of flood extent at the same time, at a comparably high resolution, and covering the same area. However, the RAPID system has already been validated in two instances: for Hurricane Harvey and for the Northwestern Floods. In the current version of the manuscript, beyond mentioning these validations, we also included a comparison with EMS maps for the Bahamas. We included the details of the validation in the Methodology section:

“The RAPID system has been quantitatively validated in past studies against manually derived flood maps using (overall, user, producer) agreement scores, representing (accuracy, true positive rate, precision) parameters of the confusion matrix. Specifically, for Hurricane Harvey, RAPID was validated against the DFO comprehensive flood map of August 30, 2017 (Shen et al., 2019) and against the USGS DSWE Northwestern flood map of June 25, 2019 (Yang et al., 2019). RAPID yielded consistently high agreement scores for Harvey (93%, 75%, 77%) and the Northwestern flood (96%, 84%, 76%). For Hurricane Dorian, we are presenting a comparison between RAPID and the Copernicus Emergency Management Service (EMS) first estimate maps (available at <https://emergency.copernicus.eu/mapping/list-of-components/EMSR385/FEP/ALL>), both derived from the Sentinel-1 SAR observations. EMS flooding maps are not available for the entire SAR images, but only for the Abaco Islands on September 2, 2019, and for Grand Bahama on September 4, 2019.”

We described the comparison between EMS and RAPID for both September 2 and September 4 in the Results section:

“The agreement (overall, user, producer) scores between RAPID and EMS flooding maps for the Abaco Islands on September 2 and September 4, derived from the confusion matrix shown in Table 1, were (77%, 90%, 41%) and (89%, 61%, 86%), respectively. The high overall and user agreement scores for the September 2 flooding are also depicted in the flood maps of Figure 2 indicating a very good overlap of the two products over the coast of Great Abaco, while the relatively low producer agreement comes from the lack of flood detection by the EMS algorithm over the multiple near-sea-surface-elevation islands, located in the front of the western coast of Great Abaco. The relatively low user agreement score between the two products on September 4 is due to the fact that RAPID classifies some non-flooded areas within the EMS flooded boundary, which are expected to occur as a consequence of the flood recession.”

Confusion Matrix		September 2 – Great Abaco		September 4 – Grand Bahama	
		EMS		EMS	
		Flooded	Non-flooded	Flooded	Non-flooded
RAPID	Flooded	2,274,927 (14.5%)	3,318,143 (21.1%)	1,880,609 (13.2%)	32,989 (2.3%)
	Non-flooded	260,335 (1.7%)	9,847,017 (62.7%)	1,219,786 (8.6%)	10,710,519 (75.9%)

Table 2: Confusion matrix between RAPID and EMS flooding products for September 2, 2019 overpass over Great Abaco (left) and for September 4, 2019 overpass over Grand Bahama (right). For each matrix, number and percentage of pixels is reported.

7. Figure 2 and 3: it would be important to describe which data source was used to separate between normal water conditions and flooding. It would be helpful to visualize layers of normal water extent in the figures.

RAPID uses dry references for change detection. We vote (some studies name it the temporal filtering technique) each pixel using multiple dry references (no less than 5 overpasses) to create a noise-free persistent water extent (normal water extent).

We added the following sentence in the Methodology section: *“In step 2, the noise-free persistent water extent (know water body) is computed using at least 5 dry overpasses for each pixel.”*

8. Line 113: Without any information about the performance of RAPID and without any reference to other approaches in flood mapping reported in the literature I would suggest to remove the sentence: “We believe its ability to map such a large area of inundation so quickly makes RAPID the fastest fully automated method for assessing flood extension”

Since in the revised version we are now providing the accuracy information of RAPID for different events, showing consistently high performance, we can safely make the conclusion. Other approaches have been extensively discussed in Shen et al., 2019a and, for brevity, cannot be discussed here.

9. Line 115: These international collaborations or mechanisms exist and the authors should refer to them (e.g. International Charter “Space and Major Disasters”, Sentinel Asia, Copernicus Emergency Management Service - Mapping).

Thank you for this comment. We included these collaborations in the revised version of our manuscript:

“This limitation can be overcome through international collaborations, such as the International Charter “Space and Major Disasters”, Sentinel Asia, NASA-ISRO SAR Mission and Copernicus Emergency Management Service – Mapping, that may increase the availability of data from other satellite missions.”

References:

- Bovolo, F., & Bruzzone, L. (2007). A split-based approach to unsupervised change detection in large-size multitemporal images: Application to tsunami-damage assessment. *IEEE Transactions on Geoscience and Remote Sensing*, 45, 1658-1670
- Chini, M., Hostache, R., Giustarini, L., Matgen, P.J.I.T.o.G., & Sensing, R. (2017). A hierarchical split-based approach for parametric thresholding of SAR images: Flood inundation as a test case, 55, 6975-6988
- Cian, F., Marconcini, M., & Ceccato, P. (2018). Normalized Difference Flood Index for rapid flood mapping: Taking advantage of EO big data. *Remote Sensing of Environment*, 209, 712-730
- Giustarini, L., Hostache, R., Kavetski, D., Chini, M., Corato, G., Schläffer, S., Matgen, P.J.I.T.o.G., & Sensing, R. (2016). Probabilistic flood mapping using synthetic aperture radar data, 54, 6958-6969
- Giustarini, L., Hostache, R., Matgen, P., Schumann, G.J.-P., Bates, P.D., & Mason, D.C. (2012). A change detection approach to flood mapping in urban areas using TerraSAR-X. *Geoscience and Remote Sensing, IEEE Transactions on*, 51, 2417-2430
- Horritt, M. (1999). A statistical active contour model for SAR image segmentation. *Image and Vision Computing*, 17, 213-224
- Horritt, M.S., Mason, D.C., Cobby, D.M., Davenport, I.J., & Bates, P.D. (2003). Waterline mapping in flooded vegetation from airborne SAR imagery. *Remote Sensing of Environment*, 271–281
- Kittler, J., & Illingworth, J. (1986). Minimum error thresholding. *Pattern recognition*, 19, 41-47

- Lu, J., Giustarini, L., Xiong, B., Zhao, L., Jiang, Y., & Kuang, G. (2014). Automated flood detection with improved robustness and efficiency using multi-temporal SAR data. *Remote Sensing Letters*, 5, 240-248
- Martinis, S., Kersten, J., & Twele, A. (2015). A fully automated TerraSAR-X based flood service. *ISPRS Journal of Photogrammetry and Remote Sensing*, 104, 203-212
- Martinis, S., Twele, A., & Voigt, S. (2009). Towards operational near real-time flood detection using a split-based automatic thresholding procedure on high resolution TerraSAR-X data. *Natural Hazards and Earth System Sciences*, 9, 303-314
- Matgen, P., Hostache, R., Schumann, G., Pfister, L., Hoffmann, L., & Savenije, H. (2011). Towards an automated SAR-based flood monitoring system: Lessons learned from two case studies. *Physics and Chemistry of the Earth, Parts A/B/C*, 36, 241-252
- Shen, X., Anagnostou, E.N., Allen, G.H., Brakenridge, G.R., & Kettner, A.J. (2019). Near Real-Time Nonobstructed Flood Inundation Mapping by Synthetic Aperture Radar. *Remote Sensing of Environment*, 221, 302-335
- Yang, Q., Shen, X., Anagnostou, E.N., Mo, C., Eggleston, J.R., & Kettner, A.J. (2019). An Unprecedented High-Resolution Flood Inundation Archive (2016-present) from Sentinel-1 SAR imageries over the CONUS. *Bulletin of American Meteorological Society*, (proposal accepted)